estimates the population relaxation rate. However, this remains under investigation.

The AT splitting and gain without inversion in the Mollow absorption spectrum imply that the absorption and gain inside a single QD are tunable. In the AT configuration, the absorption of the probe beam can be switched on and off by applying a strong optical field. In contrast, in the MAS experiment, the absorption of the frequency fixed probe beam can be tuned to be positive or negative (gain) by adjusting the pump field strength. Our results are the first step toward the realization of electromagnetically induced transparency and lasing without inversion in the spin-based lambda system and suggest that QDs offer the potential to be used as elements in optoelectronics and quantum logic devices (*4*, *27*).

Note added in proof: Since the submission of this paper, two papers have appeared on http://arxiv.org that report studies of the resonant excitation of quantum dots in the strong excitation regime. The first (*31*) reports a measurement of the fluorescence correlation function that Mollow first calculated, and the second (*32*) reports Rabi oscillations.

References and Notes

1. D. Loss, D. P. DiVincenzo, *Phys. Rev. A.* **57**, 120 (1998).
2. Z. Yuan *et al.*, *Science* **295**, 102 (2002).
3. H.-J. Briegel, W. Duer, J. I. Cirac, P. Zoller, *Phys. Rev. Lett.* **81**, 5932 (1998).
4. D. Gammon, D. G. Steel, *Phys. Today* **55**, 36 (2002).
5. L. J. Sham, T. M. Rice, *Phys. Rev.* **144**, 708 (1966).
6. V. M. Axt, A. Stahl, *Z. Phys. B* **93**, 195 (1994).
7. T. H. Stievater *et al.*, *Phys. Rev. Lett.* **87**, 133603 (2001).
8. H. Kamada, H. Gotoh, J. Temmyo, T. Takagahara, H. Ando, *Phys. Rev. Lett.* **87**, 246401 (2001).
9. H. Htoon *et al.*, *Phys. Rev. Lett.* **88**, 087401 (2002).
10. A. Zrenner *et al.*, *Nature* **418**, 612 (2002).
11. J. J. Sanchez-Mondragon, N. B. Narozhny, J. H. Eberly, *Phys. Rev. Lett.* **51**, 550 (1983).
12. J. P. Reithmaier *et al.*, *Nature* **432**, 197 (2004).
13. T. Yoshie *et al.*, *Nature* **432**, 200 (2004).
14. K. Hennessy *et al.*, *Nature* **445**, 896 (2007).
15. B. R. Mollow, *Phys. Rev.* **188**, 1969 (1969).
16. J. Dupont-Roc, G. Grynberg, C. Cohen-Tannoudji, *Atom-Photon Interactions: Basic Processes and Applications* (Wiley, New York, 1998).
17. S. H. Autler, C. H. Townes, *Phys. Rev.* **100**, 703 (1955).
18. E. V. Baklanov, V. P. Chebotaev, *Sov. Phys. JETP* **34**, 490 (1972).
19. B. R. Mollow, *Phys. Rev. A.* **5**, 2217 (1972).
20. S. Haroche, F. Hartmann, *Phys. Rev. A.* **6**, 1280 (1972).
21. F. Y. Wu, S. Ezekiel, M. Ducloy, B. R. Mollow, *Phys. Rev. Lett.* **38**, 1077 (1977).
22. M. T. Gruneisen, K. R. MacDonald, R. W. Boyd, *J. Opt. Soc. Am. B* **5**, 123 (1988).
23. S. G. Carter *et al.*, *Science* **310**, 651 (2005).
24. N. Lu, P. R. Berman, *Phys. Rev. A.* **44**, 5965 (1991).
25. Materials and methods are available as supporting material on *Science* Online.
26. D. Gammon, E. S. Snow, B. V. Shanabrook, D. S. Katzer, D. Park, *Phys. Rev. Lett.* **76**, 3005 (1996).
27. M. O. Scully, M. S. Zubairy, *Quantum Optics* (Cambridge Univ. Press, Cambridge, 1997).
28. P. Meystre, M. Sargent, *Elements of Quantum Optics* (Springer-Verlag, Heidelberg, Germany, ed. 3, 1998) chap. 9.
29. A. Thranhardt, C. Ell, G. Khitrova, H. M. Gibbs, *Phys. Rev. B* **65**, 035327 (2002).
30. A. Hogele *et al.*, *Phys. Rev. Lett.* **93**, 217401 (2004).
31. A. Muller *et al.*, http://arxiv.org/abs/0707.0656.
32. R. Melet *et al.*, http://arxiv.org/abs/0707.3061.

33. This work is supported by the U.S. Army Research Office, Air Force Office of Scientific Research, Office of Naval Research, NSA/LPS, and FOCUS-NSF.

Supporting Online Material

www.sciencemag.org/cgi/content/full/317/5840/929/DC1
Materials and Methods
SOM Text
Fig. S1
References

26 March 2007; accepted 4 June 2007
10.1126/science.1142979

Deep Ultraviolet Light–Emitting Hexagonal Boron Nitride Synthesized at Atmospheric Pressure

Yoichi Kubota,* Kenji Watanabe, Osamu Tsuda, Takashi Taniguchi

Materials emitting light in the deep ultraviolet region around 200 nanometers are essential in a wide-range of applications, such as information storage technology, environmental protection, and medical treatment. Hexagonal boron nitride (hBN), which was recently found to be a promising deep ultraviolet light emitter, has traditionally been synthesized under high pressure and at high temperature. We successfully synthesized high-purity hBN crystals at atmospheric pressure by using a nickel-molybdenum solvent. The obtained hBN crystals emitted intense 215-nanometer luminescence at room temperature. This study demonstrates an easier way to grow high-quality hBN crystals, through their liquid-phase deposition on a substrate at atmospheric pressure.

Hexagonal boron nitride (hBN) and cubic boron nitride (cBN) are known as the representative crystal structures of BN. hBN is chemically and thermally stable and has been widely used as an electrical insulator and heat-resistant material for several decades; cBN, which is a high-density phase, is almost as hard as diamond (*1*).

Promising semiconductor characteristics due to a direct band gap of 5.97 eV were recently discovered in high-purity hBN crystals obtained by a high-pressure flux method, paving the way for a material that efficiently emits deep ultraviolet (DUV) light (*2*, *3*). Similar to aluminum nitride (AlN) (*4*) and gallium nitride (GaN) (*5*), hBN may have attractive potential as a wide–band gap material. The layered structure of hBN makes the material mechanically weak, but it has greater chemical and thermal stability than GaN and AlN. The interesting optical properties of hBN, such as its huge exciton-binding energy (*2*), are due to its anisotropic structure, whereas a single crystal's basal plane in hBN is not easily broken because of its strong in-plane bonds. Thus far, the excitation of hBN by an accelerated electron beam or by far-UV light above the band-gap energy shows various efficient luminescence bands near the band edge.

However, the electronic properties of hBN near the band gap, which is fundamental information for developing DUV light–emission applications, are not yet fully understood, as seen by the fact that the origins of the luminescence bands are still controversial (*2*, *6*, *7*). Two opposed models, a Wannier exciton model and a Frenkel exciton model, have been proposed. The former model is based on results of the intrinsic absorption spectra near the band edge from pure single crystals (*2*), and the latter model is based on theoretical calculations and a luminescence study that used powder samples (*7*) showing very intense impurity bands around 4.0 eV (*8*). According to work examining the correlation between impurities and defects and luminescence properties (*8*, *9*), the intrinsic optical properties of samples are hindered by the extrinsic ones if experimenters do not have careful control of the samples' crystallinity and polymorphic purity. In (*7*), the strong 5.46-eV luminescence band, which is attributed to stacking faults (*9*), dominated in the region of the band gap, and the most intense photoluminescence band at 215 nm, observed in a pure single crystal, was not observed from the powder sample. Pure samples with high crystallinity must be indispensable for developing this new material for DUV light–emitting applications. Because high-quality hBN crystals have so far been produced only by high-pressure processes, it is important to discover an alternative synthesis scheme for conventional crystal growth at atmospheric pressure.

DUV-luminous single-crystalline hBN has been created through the reduction of O and C impurities with the use of a reactive solvent of the Ba-BN system under high pressure (*2*, *3*, *8*).

National Institute for Materials Science (NIMS), Tsukuba, Ibaraki 305-0044, Japan.

*To whom correspondence should be addressed. E-mail: kubota.yoichi@nims.go.jp

Although the Ba-BN system is a useful solvent to obtain high-purity hBN crystals under high pressure, the system cannot be used at atmospheric pressure, probably because of the decomposition of the solvent itself at high temperature. A closed high-pressure system is required for using Ba-BN as a solvent, because the Ba-BN system is unstable at high temperature and is also extremely reactive with O and in the presence of humidity at atmospheric conditions (*8*).

hBN is thermodynamically stable at high temperatures and at atmospheric pressure. Therefore, it should be possible to obtain high-quality hBN crystals at atmospheric pressure by using an appropriate solvent. Ishii and Sato reported the preparation of hBN single crystals by using a Si flux under 1 atm of N_2 (*10*). Although they claimed that the crystals showed sharp absorption near 5.8 eV, DUV-emitting properties were not observed. Because the band-edge optical properties are strongly affected by O and C impurities (*8*), the emission characteristics of their hBN crystals were probably affected by the C impurity mentioned in their report (*10*). Yano *et al*. reported the synthesis of hBN crystals using a Na solvent under 100 atm of N_2 (*11*). They observed a cathodoluminescence spectrum of the hBN with a peak near 3.8 eV and a weak emission near 5.6 eV.

A variety of solvents have been studied for cBN synthesis at high-pressure and high-temperature conditions: alkali and alkaline earth metals (*12*, *13*), their BN compounds (*3*, *8*, *14*), and some transition metals (*15*, *16*). Because a solvent useful for cBN growth may be useful for hBN growth, we focused on transition-metal solvents, which do not decompose at atmospheric pressure. We recently established a reaction diagram of Ni and BN under high pressures and found that hBN dissolves in molten Ni and precipitates as tiny cBN crystals, and also recrystallizes as hBN at high-pressure and high-temperature conditions (*17*). In the chemical vapor deposition process, Ni seems to have a catalytic action that initiates the formation of the hBN (*18*). A UV-luminous hBN layer was deposited on a Ni substrate, though the layer was not homogeneous (*19*). Yang *et al*. reported that their hBN crystals were formed from a molten surface layer of Ni substrate, although the obtained crystals were only a few micrometers in size (*20*). They did not claim any information about the optical characteristics of the products.

Here we describe the synthesis of high-quality hBN crystals under atmospheric pressure using a Ni base solvent. Although the grown crystals formed aggregates with dimensions of several hundred micrometers, intense DUV emission was observed across the entire region of the grown crystals.

Initially, we used a Ni disk as the solvent and deoxidized hBN powder as a starting material for the atmospheric-pressure synthesis of hBN (*21*). The materials were put into a crucible and heated at 1350° to 1500°C for a soak period of 12 hours in the furnace. After soaking, the furnace was cooled down at a rate of 4°C/hour to 1200°C.

Colorless and transparent crystals with a thin platelike habit were found to grow on the surface of the solidified Ni solvent. The obtained crystal surface was segmented by striae into triangular or hexagonal domains. The largest crystal was about 300 μm across, with thickness of a few micrometers. The Raman spectrum of the crystal showed a single peak at 1365 cm^{-1}, which corresponds to the in-plane vibrational mode of hBN (*22*), with full width at half maximum (FWHM) of 9.3 cm^{-1}. The yield of the reaction was, however, very low, and the recrystallized hBN was observed only on some small parts of the surface of the solvent.

The binary Ni-B and Ni-N phase diagrams show that approximately 30 weight % (wt%) B is in a liquid phase at 1550°C (*23*), whereas the solubility of N in liquid Ni is only 0.0012 wt% at 1550°C at 1 atm of N_2 (*24*). Thus the yield of recrystallized hBN is controlled by the N solubility in the liquid phase of the Ni solvent. Kowanda and Speidel reported that the N solubility of a liquid Ni-Mo alloy increases with an increasing concentration of Mo; the addition of Mo of 40 wt% to the Ni solvent enhances the solubility of N by 40 times as compared to that in the pure Ni (*24*). We thus added Mo to the Ni solvent so as to increase N content in solution.

Many faceted platelike hBN crystals were obtained on the surface of the solidified Ni-Mo solvent (Fig. 1A). The thickness of the crystals grown was typically 10 μm, as characterized by optical microscopy. The largest hBN crystal obtained in this study was on the order of 300 μm × 200 μm. We found that the crystals were aggregated and fully covered the surface of the Ni-Mo solvent, which was 20 mm in diameter (Fig. 1B, inset). Although the grown crystals fragmented into several pieces during the acid treatment, the recovered crystal was transparent, colorless, and about 9 mm × 4 mm in size (Fig. 1B). These results show that the Mo in the Ni-Mo alloy increases the yield of recrystallized hBN, probably by increasing the N solubility of the solvent.

The Raman spectrum of the crystal shows a single peak at 1365 cm^{-1} with a FWHM of 9.0 cm^{-1} (Fig. 2A). The FWHM of our high-quality hBN single crystals obtained by high-pressure and high-temperature synthesis was 9.1 cm^{-1}, suggesting that quality of the crystal from the Ni-Mo binary system was almost comparable to that of the crystal produced by high-pressure and high-temperature synthesis.

Figure 2B shows an x-ray diffraction (XRD) profile of the aggregate crystals that were ground into fine powder. All the peaks can be assigned as those of hBN (Joint Committee on Powder

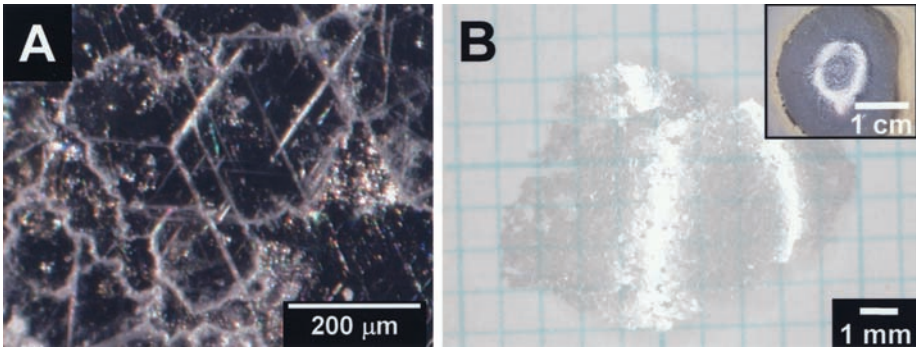

Fig. 1. Optical micrographs of recrystallized hBN obtained with a Ni-Mo solvent. (**A**) Typical hBN crystal on the solidified solvent (as grown). (**B**) A fragment of aggregate hBN crystals after acid treatment (the inset is an optical micrograph of a recovered sample). The shiny white regions are reflected light.

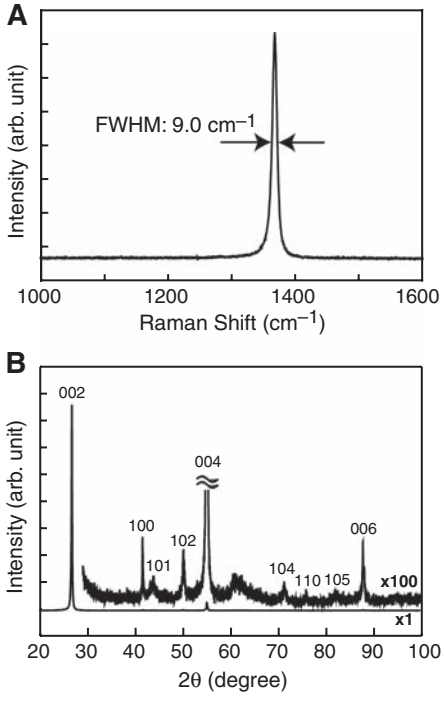

Fig. 2. Characteristics of recrystallized hBN grown in a Ni-Mo solvent at atmospheric pressure. (**A**) Raman spectrum obtained from recrystallized hBN. (**B**) X-ray diffraction profile of recrystallized hBN after being ground to fine powder. arb., arbitrary.

Diffraction Standards card no. 34-421), except the broad peak near 60°, which is attributed to the Si sample holder.

Figure 3 shows typical cathodoluminescence spectra of the hBN crystals grown with the Ni and Ni-Mo solvents. The spectra were measured at room temperature. Each spectrum exhibits an intense free-exciton luminescence peak at 215 nm that is characteristic of a high-quality hBN crystal (*2*). The shoulder structure around 227 nm, which we attribute to a bound exciton caused by a stacking disorder, is relatively low, suggesting that these crystals have low stacking disorder (*9*). We also observed weak broad bands around 300 nm, especially in the Ni solvent system, which were probably due to residual impurities such as O and C (*2*, *8*). It is known that Mo forms carbide whereas Ni does not (*25*, *26*), suggesting that Mo could play the role of the C getter in the Ni solvent. The reduction of C impurities in the crystals was achieved, as suggested by the less-broadband feature near 300 nm. The dominant DUV band near the band edge at 215 nm reveals the low impurity content of our crystals.

Our results show that the atmospheric-pressure Ni-Mo solvent system is as effective for the synthesis of high-quality hBN as are high-pressure and high-temperature solvent systems. We made direct quality comparisons of the emission characteristics of the samples grown in this study and those grown at high pressures. The band-edge emission intensities of the both crystals were of similar order (Fig. 3C).

hBN recrystallization using a metal solvent can lead to large-area deposition of high-quality hBN crystals on a substrate with the use of a liquid-phase epitaxy process under atmospheric-pressure conditions. In order to examine the growth of a hBN crystal on a substrate from the solution, we added a sapphire substrate to the starting materials and applied the same growth process as above, using the Ni-Mo solvent. We observed that hBN crystals with smooth surfaces grew on the substrate (Fig. 4A). The cathodoluminescence spectrum of the hBN crystals showed the similar dominant luminescence band at 215 nm (Fig. 3). Figure 4B shows the intense 215-nm luminescence image at room temperature corresponding to Fig. 4A. The intensity of the 215-nm band is uniform over almost all of the surface. The cathodoluminescence image of striae is substantially enhanced by the scattered 215-nm luminescence in Fig. 4B.

When Mo was added to the Ni solvent, the yield of recrystallized hBN was substantially increased because of the enhancement of N solubility in the Ni-Mo system. The grown hBN crystals were of very high quality, exhibiting their band-edge optical nature of intense 215-nm luminescence. Consequently, we can establish an alternative synthesis route for large amounts of high-quality hBN crystals, as well as their liquid-phase deposition process on a substrate at atmospheric pressure.

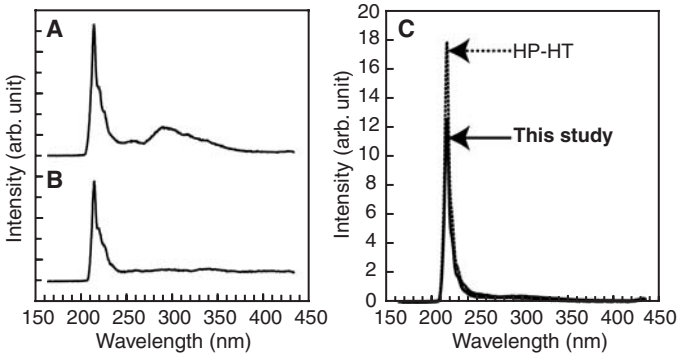

Fig. 3. Cathodoluminescence spectra of recrystallized hBN at room temperature. (**A**) hBN obtained with a Ni solvent. (**B**) hBN obtained with a Ni-Mo solvent. (**C**) Direct quality comparison of the emission characteristics. Solid line, hBN obtained with a Ni-Mo solvent at atmospheric pressure (in this study); dotted line, hBN obtained with a Ba-BN solvent at high pressure and high temperature (HP-HT).

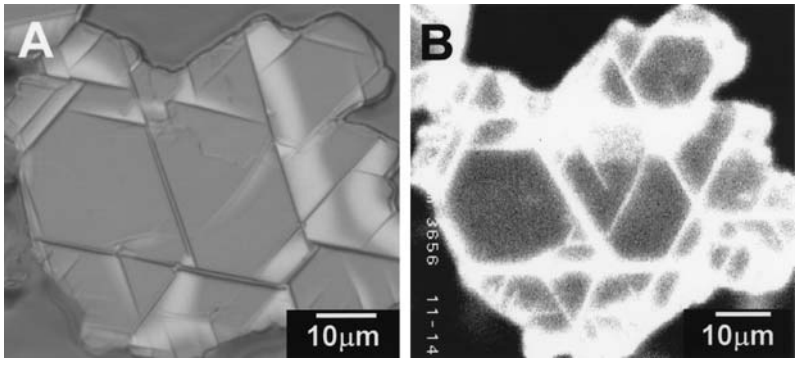

Fig. 4. Images of hBN crystal grown on the *a*-plane sapphire substrate (obtained with a Ni-Mo solvent prepared at 1400°C). (**A**) Differential interference microscopic image. (**B**) Cathodoluminescence image for 215-nm band. We did not find any intensity change of the measured spectra between the grain boundary and the plane surface area when measuring the point-to-point mode of the cathodoluminescence system, where the electron beam remained stationary and the measured luminescence was confined to the exposed spot area.

References and Notes

1. O. Mishima, K. Era, in *Electric Refractory Materials*, Y. Kumashiro, Ed. (Dekker, New York, 2000), chap. 21.
2. K. Watanabe, T. Taniguchi, H. Kanda, *Nat. Mater.* **3**, 404 (2004).
3. T. Taniguchi, K. Watanabe, S. Koizumi, *Phys. Status Solidi A* **201**, 2573 (2004).
4. Y. Taniyasu, M. Kasu, T. Makimoto, *Nature* **441**, 325 (2006).
5. I. Akasaki, H. Amano, *Jpn. J. Appl. Phys.* **36**, 5393 (1997).
6. B. Arnaud, S. Lebegue, P. Rabiller, M. Alouani, *Phys. Rev. Lett.* **96**, 026402 (2006).
7. M. G. Silly *et al.*, *Phys. Rev. B* **75**, 085205 (2007).
8. T. Taniguchi, K. Watanabe, *J. Cryst. Growth* **303**, 525 (2007).
9. K. Watanabe, T. Taniguchi, T. Kuroda, H. Kanda, *Appl. Phys. Lett.* **89**, 141902 (2006).
10. T. Ishii, T. Sato, *J. Cryst. Growth* **61**, 689 (1983).
11. M. Yano *et al.*, *Jpn. J. Appl. Phys.* **39**, L300 (2000).
12. R. H. Wentorf Jr., *J. Chem. Phys.* **34**, 809 (1961).
13. T. Endo, O. Fukunaga, M. Iwata, *J. Mater. Sci.* **14**, 1375 (1979).
14. R. C. DeVries, J. F. Fleisher, *J. Cryst. Growth* **13–14**, 88 (1972).
15. H. Saito, M. Ushio, S. Nagano, *Yogyo Kyokai Shi* **78**, 1 (1970) [in Japanese with an English abstract].
16. T. Taniguchi, *New Diamond Front. Carbon Technol.* **14**, 289 (2004).
17. Y. Kubota, K. Watanabe, T. Taniguchi, *Jpn. J. Appl. Phys.* **46**, 311 (2007).
18. T. Takahashi, H. Itoh, A. Takeuchi, *J. Cryst. Growth* **47**, 245 (1979).
19. O. Tsuda, K. Watanabe, T. Taniguchi, *Jpn. J. Appl. Phys.* **46**, L287 (2007).
20. P. C. Yang, J. T. Prater, W. Liu, J. T. Glass, R. F. Davis, *J. Electron. Mater.* **34**, 1558 (2005).
21. Materials and methods are available as supporting material on *Science* Online.
22. R. Geick, H. Perry, *Phys. Rev.* **146**, 543 (1966).
23. P. K. Liao, K. E. Spear, in *Binary Alloy Phase Diagrams*, T. B. Massalski, Ed. (ASM International, Materials Park, OH, ed. 2, 1990), vol. 1, pp. 508–510.
24. C. Kowanda, M. O. Speidel, *Scripta Mater.* **48**, 1073 (2003).
25. T. B. Massalski, in *Binary Alloy Phase Diagrams*, T. B. Massalski, Ed. (ASM International, Materials Park, OH, ed. 2, 1990), vol. 1, pp. 861–862.
26. M. F. Singleton, P. Nash, in *Binary Alloy Phase Diagrams*, T. B. Massalski, Ed. (ASM International, Materials Park, OH, ed. 2, 1990), vol. 1, pp. 866–867.

27. The authors thank T. Wada of NIMS for his support in the XRD study. This study was supported by a Grant-in-Aid for Scientific Research of the Japan Society for the Promotion of Science (nos. 19205026 and 18360321).

Supporting Online Material

www.sciencemag.org/cgi/content/full/317/5840/932/DC1
Materials and Methods
Fig. S1
References

24 April 2007; accepted 22 June 2007
10.1126/science.1144216